

## Measurements-based Method for Impedance Characterization of Residential Loads

Despina Anastasiadou<sup>1</sup> and Theodore Antonakopoulos<sup>2</sup>

<sup>1</sup>Research Academic Computers Technology Institute,  
61 Riga Feraiou Str. – 26100 Patras, Greece  
Phone: +30-2610-996-489, Fax: +30-2610-997-342, E-mail: Despina.Anastasiadou@cti.gr.

<sup>2</sup>Department of Electrical Engineering and Computers Technology  
University of Patras, Rio, Patras – 26500, Greece  
Phone: +30-2610-996-487, Fax: +30-2610-997-342, E-mail: antonako@ee.upatras.gr.

**Abstract** – *The issue of load impedance characterization in the residential environment is addressed in this work. The transfer function of any point-to-point link on any indoor power line network depends on the communications characteristics of the medium and the presence of residential loads, in the form of electrical appliances. Measurements of the transfer function variations on an experimental set-up, caused by an unknown residential load, can be exploited to determine the value of its impedance. In this paper, we propose two new methods of impedance identification and analyze their accuracy and performance limitations.*

**Keywords** – *Power-line Communications, System Identification, Impedance Measurements.*

### I. INTRODUCTION

In a time of increasing demand for broadband communications services in the Home/Office environment, the idea of transforming the indoor power grid, from a purely mains distribution network, into a medium delivering high speed data services, appears particularly attractive. The motivation for such an aspiring effort originates from its ubiquitous node availability, even in areas with limited twisted-pair and coaxial cable installations and poor radio coverage, which makes the indoor power grid a potentially convenient and inexpensive "no new wires" candidate for data transmission. Consequently, during the last few years, focus has been placed on the development of sophisticated transmission techniques, in order to mitigate the influence of the principal impairments on power line channels: varying attenuation, multipath frequency-selective fading, multiple access interference, background and impulsive noise. It is, therefore, justified to consider that gathering information about the factors that cause the power grid's unfavorable behavior is critical to the development of reliable high speed data communications algorithms.

The indoor power line network has been characterized as a multipath propagation environment, whose response can be traced back to its topology, cable properties and termination loading. It is vital to recognize the indoor electrical loads (in

the form of appliances connected to the AC outlets) as the sources of various disturbances and the cause for the network's time varying characteristics. This conclusion is drawn from the observation that the loads are the main varying factor in the power line communications environment, since they may change the location of their connection or alter their impedance characteristics during operation. Ample information can be found in the literature regarding the characterization of several residential appliances as sources of disturbance [1], [2], [3]. On the contrary, investigation of their impedance as a function of frequency is very limited [4], [5]. This task is mainly hindered by the presence of the mains voltage, when performing measurements on operating appliances.

In this work, we propose two new heuristic methods of load impedance characterization in the residential environment. The proposed methods are based on time domain measurements, performed on a suitable experimental set-up. The acquired measurement results are processed using algorithms, specifically developed for power line channel identification and impedance load estimation.

In the following section the measurement setup is described and details are offered on the measurement methodology. Section III elaborates on the algorithms of data processing that lead to the impedance characterization of the load under measurement, while section IV presents an insightful analysis on the procedures' accuracy, limitations and experimental results.

### II. EXPERIMENTAL SETUP AND MEASUREMENT METHODOLOGY

The proposed methodology of load impedance estimation is based on the concept of using the measured response of a low-complexity power line topology, where the unknown load is connected, along with its analytically calculated equivalent to estimate the undefined impedance. Therefore, the procedure is primarily divided into the measurement and the post-processing stage.

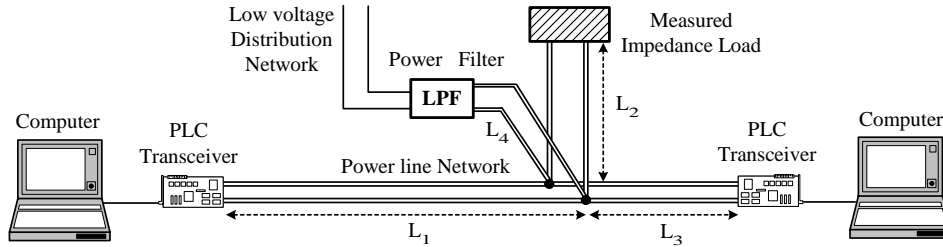


Fig. 1. The experimental measurement setup.

The measurement setup used in our methodology is based on the experimental network presented in Fig. 1. The network comprises four line sections of particular lengths, connected to a common junction. It is constructed using common residential power line cables, whose communication properties, namely the characteristic impedance  $Z_0$  and the propagation constant  $\gamma$ , must be known in advance. The network is supplied with 230V AC through a high-current passive low pass filter (LPF), connected to one of its termination points, which isolates the experimental setup from external interference. Two of the remaining terminations function as the measurement system's input and output nodes, where the power line communications (PLC) transceivers are connected. The transceivers include suitable coupling circuits for their connection to the power grid. The coupling circuits exhibit flat response and linear phase in the frequency band of interest and their impedance characteristics are well defined. The transceivers communicate with local processing units, which perform generation of the input data sequences and post processing of the received channel output sequences. Finally, the load under measurement terminates the remaining line section.

The line section lengths have been properly selected in order to facilitate the measurement analysis. In particular, the following issues were addressed through the appropriate selection of cable lengths:

- The low pass power filter exhibits minimal impedance characteristics (almost as a short circuit in the MHz band), and therefore its effect on the signal propagation paths need to be minimized through a relatively long cable connection.
- The line section lengths should be chosen with regard to the cable's properties, so that the number of significant propagation paths is minimized to aid the calculations involved in the estimation algorithm.

The data sequences, used for executing the experimental measurements, are carefully generated in order to ensure the desired accuracy on the estimation of the measured impedance load. Due to the channel's frequency selective behavior, the measurement and estimation process takes into consideration that the frequency band of interest has to be divided into a number of consecutive subchannels. The bandwidth of each subchannel is selected so that the network's response is practi-

cally constant in the respective frequency range. The level of this constant response depends on the impedance of the connected load. Therefore, the generated sequences were confined to each subchannel's frequency range, to ensure that the system's excitation is limited to the corresponding band.

### III. IMPEDANCE LOAD ESTIMATION ALGORITHMS

Impedance estimation of the load under measurement is based on an analytical method of calculating the power line channel's response by analyzing it as a multipath propagation environment [6]. The analysis relates the frequency selective channel behavior to the network's topology, the cable's physical properties and the termination loading.

Prior to the discussion on the algorithm's details, we briefly describe the analytical process through which the indoor power line network is modelled as a multipath propagation environment, where delayed replicas of the transmitted signal reach the receiver with different amplitude and phase characteristics. These multipath signal components are caused by reflections on channel discontinuities, such as termination loads and line junctions. Analytical calculation of the multipath effect in the indoor power grid is feasible due to its loop-free topology and its bounded complexity. Thus, the multipath effect can be related to the channel's physical characteristics by calculating cable loss, reflection and transmission coefficients. Considering  $L$  different propagation paths between any two communicating devices, the channel impulse response can be calculated as the sum of the received signal components, according to:

$$h(\tau, t) = \sum_{i=1}^L \{r_i e^{j\theta_i} \cdot e^{-\alpha l_i} \cdot \delta(t - \tau_i)\} \quad (1)$$

where  $r_i e^{j\theta_i}$  is the complex reflection factor of path  $i$ ,  $e^{-\alpha l_i}$  is the propagation loss factor, which depends on the path's length  $l_i$  and the propagation constant  $\gamma = \alpha + j\beta$ , and  $\tau_i = l_i/v$  is the path's delay, based on the group velocity of propagation  $v = \omega/\beta$ . The reflection factor is the product of all reflection/transmission coefficients on path  $i$ .

Although the propagation paths contributing to the channel's output are theoretically infinite ( $L \rightarrow \infty$ ), considering a more practical point of view, it can be deduced that as the

length of a path increases, more reflections occur, the attenuation level rises and therefore, the path's contribution to the overall received signal decreases. As a result, the multipath effect can be bounded to a finite number of significant paths. Selection of this number is based on a component power criterion: we consider the total signal power, calculated using a very large number of paths ( $L_{max}$ ) and select the first  $L$  paths to reach the receiver as significant, when their aggregate power is at least equal to a predefined threshold level (e.g. 96%) [1], when compared to the total power:

$$\frac{\sum_{i=1}^L |h_i|^2}{\sum_{i=1}^{L_{max}} |h_i|^2} \geq 0.96 \quad (2)$$

where  $h_i$  is the multipath component that corresponds to the  $i^{th}$  path and  $|h_i|^2$  is its power magnitude.

Since the factors involved in (1) comprise frequency dependent variables, each specific frequency corresponds to an individual response of this form. Therefore, we may conclude that the frequency response of any point-to-point communications channel can be modelled as the sum of FIR filters with complex coefficients. The filters' order depends on the line section lengths, the propagation characteristics ( $Z_0, \gamma$ ) and the selected sampling frequency.

Two main heuristic approaches on the channel estimation procedure are described in this section. Both approaches are based on the experimental results, collected using the setup presented in the previous section. The first approach is based on the ability to describe the channel's behavior, in each particular subchannel, as a time domain tap delay filter. The measurement data are used to identify the channel's impulse response corresponding to each subchannel, while the algorithm performs an analytical calculation of its impulse response, excluding the effect of the load under measurement. Comparison of the two sets of response coefficients offers adequate information in order to estimate the load's impedance.

The second approach does not depend on the identification of the channel's impulse response, but solves an analytical equation, based on the measurement data and the coefficients that correspond to the significant propagation paths. Using an iterative algorithm, the number of significant paths are identified and the converging solution is selected as the final estimation of the load's impedance. Details on both approaches are given in the following subsections.

#### A. Impulse response identification approach

The *impulse response identification approach* is based on the analytical calculation of network's impulse response, in each particular subchannel in the frequency band of interest. The first step of this method uses an autoregressive moving average (ARMAX) identification process on the input-output

data sequences. The ARMAX ( $n_a, n_b, n_c$ ) model parameters, described in (3), are estimated using the least-squares criterion:

$$A(q)y(t) = B(q)u(t) + C(q)e(t) \quad (3)$$

where  $q^{-1}u(t) = u(t-1)$ ,  $A(q) = 1 + a_1q^{-1} + \dots + a_{n_a}q^{-n_a}$ ,  $B(q) = 1 + b_1q^{-1} + \dots + b_{n_b}q^{-n_b}$ ,  $C(q) = 1 + c_1q^{-1} + \dots + c_{n_c}q^{-n_c}$  and  $u(t), y(t), e(t)$  represent the system's input, output and noise sequences respectively.

Since the residential power line channel can be described by an FIR model for each subchannel, it is valid to consider  $n_a = 0$ . Selection of a suitable order  $n_b$  is based on performing an analytical estimation of the system's order and setting  $n_b$  to be larger than any worst case projection: since in our experimental setup the topology, wiring and transceiver impedances are known, we use the analytical calculation method of [6] in order to estimate the channel's impulse response when a variety of known impedances are connected in place of the load under measurement. Therefore, we derive an estimation of the expected system order, which can be used in the identification process.

Using the analytical calculation of the channel's response for a known connected impedance, we can generate a '*partial*' response by excluding all the path coefficients that involve reflections on the connected load. The remaining impulse response coefficients represent the various propagation paths on the network that are not affected by the measured impedance load. It is clear that the value of the known impedance used in the initial calculations is irrelevant to the estimation accuracy. Comparing this '*partial*' analytical response with the '*estimated*' impulse response obtained through the measurement and identification process, we derive the impulse response coefficients, referred to as '*load inclusive*', which represent paths with reflections on the connected load. Each of these coefficients corresponds to the difference between an '*estimated*' and a '*partial*' coefficient of the same propagation delay. Using the propagation delay to identify the path (signal itinerary on the network) related to each '*load inclusive*' coefficient, we form an equation, which can be used to estimate the load's reflection coefficient and consequently its impedance. The impulse response comparison is illustrated in the diagram of Fig. 2, while the algorithm's flowchart is presented in Fig. 3.

For clarification purposes, we present a possible form of such an equation. Assuming that the first '*load inclusive*' coefficient ( $\Delta_1$ ) corresponds to the first propagation path that involves a single reflection on the load under measurement ( $p_1 : T_1 - C_1 - T_3 - C_1 - T_2$ ), the derived equation is:

$$\Delta_1 = \tau_{C_1} \cdot \rho_{T_3} \cdot \tau_{C_1} \cdot \tau_{T_2} \cdot e^{-\alpha l_{p_1}} \quad (4)$$

where  $\tau_x$  and  $\rho_x$  are the transmission and reflection coefficients at the network point indicated by index  $x$  and  $l_{p_1}$  is the path's length.

Solving the equation produces a value for the load's reflection coefficient and therefore, using (5), its impedance is estimated.

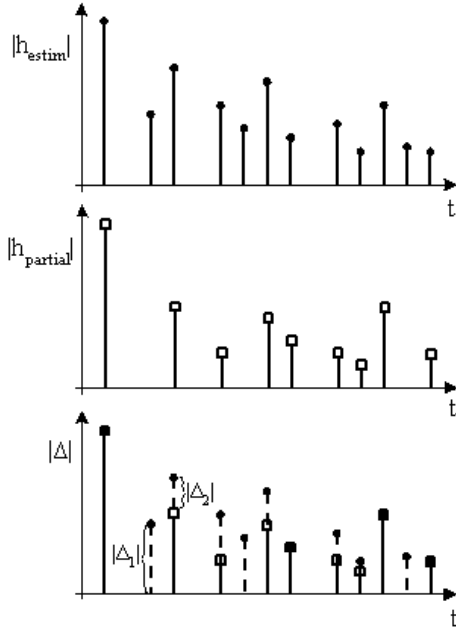


Fig. 2. 'Estimated' and 'partial' impulse response comparison.

$$Z_L = \frac{1 + \rho_{T_3}}{1 - \rho_{T_3}} \cdot Z_0 \quad (5)$$

### B. Summed propagation components approach

The *summed propagation components approach* is based on measuring the channel's transfer function in each frequency subchannel and forming an equation relating it to the analytical sum of signal components. The frequency response equivalent of (1) for a subchannel with index  $n$  is given by:

$$H_n = \sum_{i=1}^L \{r_{in} e^{j\theta_{in}} \cdot e^{-\gamma_n l_i}\} \quad (6)$$

In this expression  $H_n$  represents the frequency ratio of the output signal to the incoming signal at the channel's input. The voltage waveform measured at the transmitter point represents the signal components reaching the input point through multiple reflections on the network's discontinuities and should be properly transformed to generate the value of the incoming channel input signal. This transformation depends on the particular circuitry of the transmitter and it is explained in [6]. For the purposes of this work, we may consider that the measured transfer function  $\hat{H}_n$  is related to the above channel response  $H_n$  through a suitable voltage transformation factor, referred to as  $g_{H_n}$ .

In the signal components' sum, every coefficient is predefined except from the load's reflection coefficient. Therefore, we form a polynomial equation of the unknown  $\rho_{T_3}$ , whose degree depends on the number of reflections on the load included in the considered signal components. Since the number of

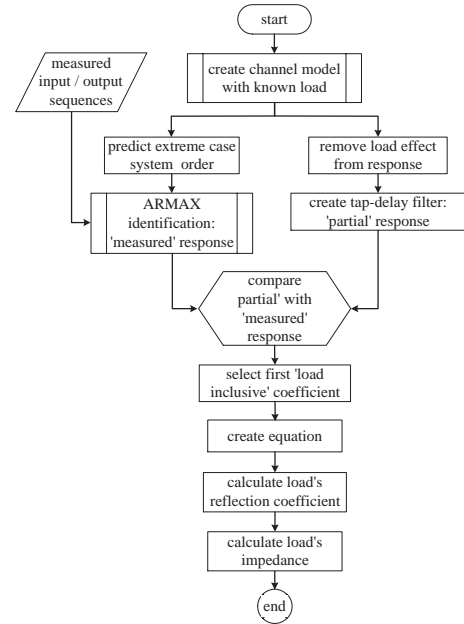


Fig. 3. Flowchart of the impulse response identification approach.

significant paths depends on the load's impedance, we use an iterative algorithm that begins by including  $L_x$  components in the equation and increases this number until one of the calculated solutions converges to a particular value. The solution that finally converges is selected as the load's reflection coefficient and its impedance is calculated using (5).

As an example, we take into consideration three propagation paths ( $p_1 : T_1 - C_1 - T_2$ ,  $p_2 : T_1 - C_1 - T_3 - C_1 - T_2$  and  $p_3 : T_1 - C_1 - T_3 - C_1 - T_3 - C_1 - T_2$ ), which are assumed to be the first in order of arrival and generate the following equation:

$$\hat{H}_n = g_{H_n} \cdot \{ \tau_{C_1} \cdot \tau_{T_2} \cdot e^{-\gamma_n l_{p_1}} + \tau_{C_1}^2 \cdot \rho_{T_3} \cdot \tau_{T_2} \cdot e^{-\gamma_n l_{p_2}} + \tau_{C_1}^3 \cdot \rho_{T_3}^2 \cdot \tau_{T_2} \cdot e^{-\gamma_n l_{p_3}} \} \quad (7)$$

This equation is used to determine the possible solutions for the reflection coefficient ( $\rho_{T_3}$ ). The iterative process will increase the number of considered paths until one of the solutions is repeatedly validated, due to its convergence to a final value, which will be used to calculate the load's impedance.

## IV. PERFORMANCE RESULTS

In this section, we analyze both impedance characterization approaches in terms of accuracy and performance limitations. Before we discuss each approach individually, it is useful to make a comment that applies to the load identification procedure, regardless of the algorithm used. The proposed impedance estimation method depends on relating the measured response to its theoretical equivalent, which leads to an irrefutable dependence of the method's accuracy on the precision with which the cable's properties ( $Z_0, \gamma$ ) are defined.

Therefore, prior to the application of the load characterization procedure, steps should be taken to determine and properly calibrate the values of  $Z_0$  and  $\gamma$  that will be used in the calculations. Identification of a cable's transmission properties is a subject of significant complexity and is covered in [7].

The *impulse response identification approach* offers results with a level of accuracy that depends on parameters such as the utilized sampling rate, the characteristics of the input data sequences and the impedance of the load under measurement itself. To offer a comprehensive analysis on the method's efficiency, we present results on the effect of such parameters on the impedance estimation. Multi-sine signals with carefully selected phases are considered highly appropriate for system identification in a narrow frequency band [8]. However, it has been observed that a considerably large length of data sequences is necessary to obtain an acceptable level of estimation accuracy. Therefore, we utilized filtered CAZAC (*constant amplitude zero autocorrelation*) sequences as excitation [9]. It was concluded that a significantly smaller number of samples was needed in order to achieve the desired system identification accuracy.

The results presented in this section, were obtained for CAZAC sequences with  $M = 499$ ,  $L = 1999$ , repeated 8 times to produce a periodical sequence of about  $16k$  samples. Each subchannel measurement sequence was created by filtering the initial broadband sequence with a high order passband FIR filter, at the corresponding frequency range, and rejecting the initial transient part of the generated sequence. Considering  $e(t) = 0$  (practically valid in a controlled and isolated measurement environment), we examined the effect of the sampling frequency ( $F_s$ ) on the impedance estimation results. It is noted that the sampling interval ( $T_s$ ) is directly related to the smallest identifiable reflection coefficient angle, since a phase shift of one degree ( $\angle 1^\circ$ ) imposed by a reflection on an unmatched load, corresponds to a time delay of  $1/(2\pi f_i)$ , where  $f_i$  is the subchannel's center frequency. The estimation error on the coefficient's angle affects the estimated impedance load ( $Z_L$ ). The extent of this effect depends on the load's impedance and  $Z_0$ . The above conclusions can be derived by observing Fig. 4, which presents the error on the estimated impedance ( $e_{Z_L}$ ), as a function of the impedance value, for three sampling frequencies (50, 70 and 100 MHz). The estimation error is calculated according to:

$$e_{Z_L} = \frac{\|Z_L - \hat{Z}_L\|^2}{\|Z_L\|^2} \quad (8)$$

This figure illustrates the importance of a high sampling frequency in order to minimize the estimation errors. The errors for  $F_s = 100$  MHz are less than 1%, while for  $F_s = 50$  MHz they reach up to a level of 3.2%. It is also evident that loads with impedance values significantly smaller than  $Z_0$  exhibit lower accuracy of estimation.

The *summed propagation components approach* may utilize tones to identify the channel's response in each subchannel.

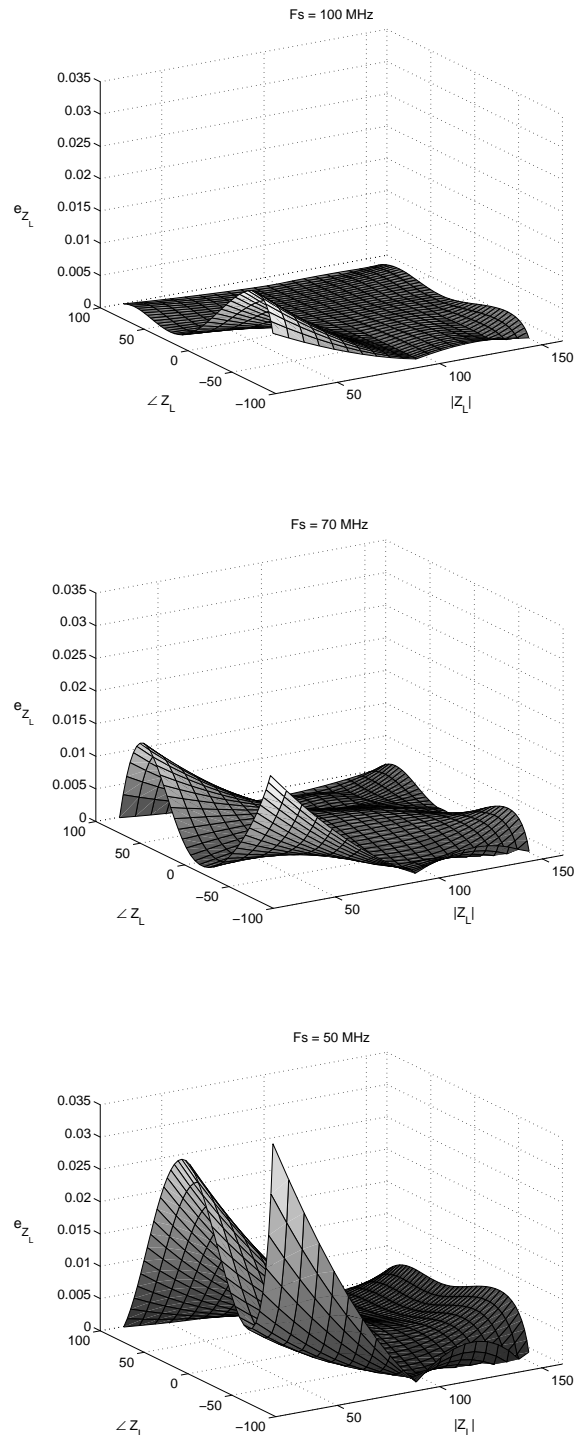


Fig. 4. Impedance estimation errors for various sampling frequencies.

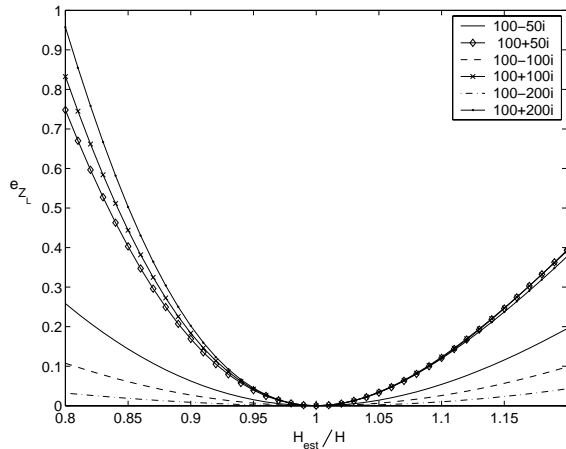


Fig. 5. Estimation error in terms of transfer function variations.

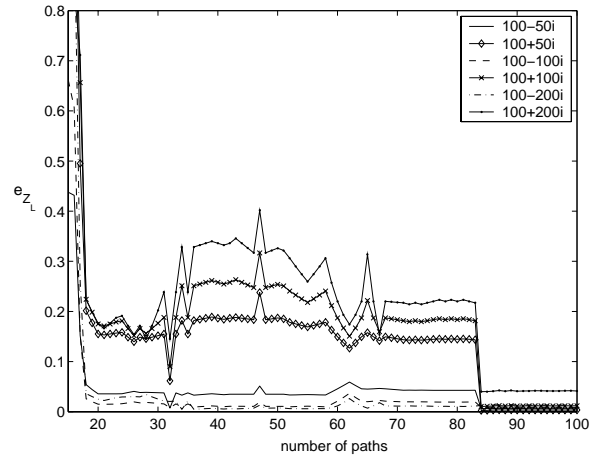


Fig. 6. Estimation error in terms of number of calculated paths.

The method uses an  $N$ -point FFT to produce the frequency domain input and output values from the corresponding measurements. Provision should be made in order to represent each frequency point with an individual FFT sample. The ratio of the  $n^{\text{th}}$  FFT sample of the output to the respective FFT sample of the input defines the channel's estimated transfer function. The method is independent of the tone sequences' length, although, in a noisy environment, averaging over a large number of  $N$  data blocks may improve the estimation results.

In Fig. 5, the load's impedance estimation errors, according to (8), are presented as a function of the deviation of the estimated transfer function ( $H_{est}$ ) from its theoretical equivalent ( $H$ ) for a particular subchannel. The various curves correspond to values of the load's impedance that exhibit different ratios between their real and imaginary parts. It can be deduced that the more inductive the load is, the lower the estimation accuracy drops.

Finally, Fig. 6 presents the impedance estimation errors as a function of the number of paths considered in the estimation equation (as in (7)). It is clearly observed that, in every impedance case, the error converges to a final minimum value as the number of paths increases. Occasional intense variations of the estimation errors are attributed to the contribution of paths that include reflections on the filter, and therefore depend on the characteristics of the specific topology.

## V. CONCLUSIONS

In order to design and improve the performance of high speed PLC systems, the sources of signal impairment and noise insertion should be identified and confronted. Impedance loads in the residential environment have a significant effect on the channel's response by creating propagation discontinuities and causing its time varying behavior.

The presented estimation methodologies facilitate the impedance characterization of various indoor loads (appli-

ances) in any frequency band of interest. The importance of this contribution lies in the fact that the utilized measurement approach enables estimation of the load's behavior while it is connected to the power distribution grid. The proposed estimation process can be used to create a database of characterized residential appliances in the high frequency range, which could be valuable information for *in situ* power line modem configuration.

## ACKNOWLEDGMENTS

This work was partially supported by the "Karatheodoris" R&D program of the University of Patras and Project 00BE23 entitled 'High Speed Transmission Technology over Residential Power Lines' of the Greek Ministry of Industry.

## References

- [1] D. Liu, B. Flint, B. Gaucher and Y. Kwark, "Wide Band AC Power Line Characterization," *IEEE Trans. Consumer Electronics*, vol.45, no. 4, pp. 1087-1097, 1999.
- [2] H. Philips, "Performance Measurements of Powerline Channels at high Frequencies," *Proc. ISPLC'98*, Tokyo, Japan, pp. 229-237, 1998.
- [3] M. Zimmermann and K. Dostert, "Analysis and Modeling of Impulsive Noise in Broad-band Powerline Communications," *IEEE Trans. Electromagnetic Compatibility*, vol.44, no. 1, pp. 249-258, Feb. 2002.
- [4] R. M. Vines, H. J. Trussell, K. C. Shuey and J. B. O'Neal, "Impedance of the Residential Power-Distribution Circuit," *IEEE Trans. Electromagnetic Compatibility*, vol.27, no. 1, pp. 6-12, Feb. 1985.
- [5] S. Tsuzuki, S. Yamamoto, T. Takamatsu and Y. Yamada, "Measurement of Japanese Indoor Power-line Channel," *Proc. ISPLC'01*, Malm, Sweden, pp. 79-84, 2001.
- [6] D. Anastasiadou and T. Antonakopoulos, "Multipath Characterization of Indoor Power Line Networks," accepted for publication in *IEEE Trans. Power Delivery*, 2004.
- [7] D. Anastasiadou and T. Antonakopoulos, "An Experimental Method of Estimating the Transmission Characteristics of Power-line Cables," *Proc. ISPLC'04*, Zaragoza, Spain, 2004.
- [8] Piet. M. T. Broersen and Stijn. de Waele, "Generating Data with Prescribed Power Spectral Density," *IEEE Trans. Instrumentation and Measurement*, vol.52, no. 4, pp. 1061-1067, Aug. 2003.
- [9] N. Benvenuto and G. Cherubini, *Algorithms for Communications Systems and their Applications*, John Wiley and Sons Ltd, 2002